

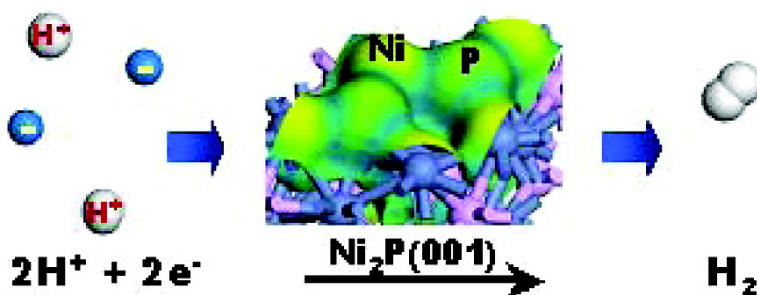
Article

Catalysts for Hydrogen Evolution from the [NiFe] Hydrogenase to the NiP(001) Surface: The Importance of Ensemble Effect

Ping Liu, and Jos A. Rodriguez

J. Am. Chem. Soc., **2005**, 127 (42), 14871-14878 • DOI: 10.1021/ja0540019 • Publication Date (Web): 01 October 2005

Downloaded from <http://pubs.acs.org> on March 25, 2009



More About This Article

Additional resources and features associated with this article are available within the HTML version:

- Supporting Information
- Links to the 9 articles that cite this article, as of the time of this article download
- Access to high resolution figures
- Links to articles and content related to this article
- Copyright permission to reproduce figures and/or text from this article

[View the Full Text HTML](#)

Catalysts for Hydrogen Evolution from the [NiFe] Hydrogenase to the Ni₂P(001) Surface: The Importance of Ensemble Effect

Ping Liu and José A. Rodriguez*

Contribution from the Department of Chemistry, Brookhaven National Laboratory, Building 555, Upton, New York 11973

Received June 16, 2005; E-mail: rodriguez@bnl.gov

Abstract: Density functional theory (DFT) was employed to investigate the behavior of a series of catalysts used in the hydrogen evolution reaction (HER, $2\text{H}^+ + 2\text{e}^- \rightarrow \text{H}_2$). The kinetics of the HER was studied on the [NiFe] hydrogenase, the $[\text{Ni}(\text{PS}3^*)(\text{CO})]^{1-}$ and $[\text{Ni}(\text{PNP})_2]^{2+}$ complexes, and surfaces such as Ni(111), Pt(111), or Ni₂P(001). Our results show that the [NiFe] hydrogenase exhibits the highest activity toward the HER, followed by $[\text{Ni}(\text{PNP})_2]^{2+} > \text{Ni}_2\text{P} > [\text{Ni}(\text{PS}3^*)(\text{CO})]^{1-} > \text{Pt} > \text{Ni}$ in a decreasing sequence. The slow kinetics of the HER on the surfaces is due to the fact that the metal hollow sites bond hydrogen too strongly to allow the facile removal of H₂. In fact, the strong H–Ni interaction on Ni₂P(001) can lead to poisoning of the highly active sites of the surface, which enhances the rate of the HER and makes it comparable to that of the [NiFe] hydrogenase. In contrast, the promotional effect of H-poisoning on the HER on Pt and Ni surfaces is relatively small. Our calculations suggest that among all of the systems investigated, Ni₂P should be the best practical catalyst for the HER, combining the high thermostability of the surfaces and high catalytic activity of the [NiFe] hydrogenase. The good behavior of Ni₂P(001) toward the HER is found to be associated with an ensemble effect, where the number of active Ni sites is decreased due to presence of P, which leads to moderate bonding of the intermediates and products with the surface. In addition, the P sites are not simple spectators and directly participate in the HER.

I. Introduction

Hydrogen production has attracted considerable attention recently with the increasing interest in hydrogen as an environmentally acceptable, alternative energy carrier.¹ Photoconversion of water to hydrogen is seen as the preferable solution. This process includes the hydrogen evolution reaction (HER), where protons and electrons are converted into hydrogen gas ($2\text{H}^+ + 2\text{e}^- \rightarrow \text{H}_2$) at the electrode surface, and Pt is usually selected as the electrode catalyst.² With the hydrogen economy approaching, there has been continuous searching for a more efficient and less expensive catalyst to replace Pt.

Hydrogenase enzymes are quite interesting because they are able to catalyze the HER and its reverse with rapid rates at room temperature.^{3–9} There are three kinds of hydrogenases that can be distinguished by their metal content: [NiFe] hydrogenases, which contain at least a Ni and an Fe atom,^{4–9} Fe-only hydrogenases with one or two Fe atoms,³ and metal-free

hydrogenases.¹⁰ Among those, [NiFe] hydrogenases represent the largest class.¹¹ The particular interest in these systems arises from the fact that the enzyme relies exclusively on available active sites.^{5,7–9} Even though extensive efforts have been made, it remains uncertain whether the active sites are Fe,⁸ Ni,⁹ or both.^{7b} In addition, the behavior of the hydrogenases has also fueled intensive research aimed at the synthesis of close molecular mimics that can achieve a comparable catalytic activity.^{3,12–16} $[\text{Ni}(\text{PNP})_2]^{2+}$ and $[\text{Ni}(\text{PS}3^*)(\text{CO})]^{1-}$ complexes are two examples of analogues of the [NiFe] hydrogenases with

- (1) Service, R. F. *Science* **2004**, *305*, 958.
- (2) Christmann, K. In *Frontiers in Electrochemistry*; Lipkowsky, J., Ross, P. N., Eds.; Wiley: New York, 1998; Vol. 1.
- (3) Tard, C.; Liu, X. M.; Ibrahim, S. K.; Bruschi, M.; De Gioia, L.; Davies, S. C.; Yang, X.; Wang, L. S.; Sawers, G.; Pickett, C. J. *Nature* **2005**, *433*, 610.
- (4) Leger, C.; Dementin, S.; Bertrand, P.; Rousset, M.; Guigliarelli, B. *J. Am. Chem. Soc.* **2004**, *126*, 12162.
- (5) Lamle, S. E.; Albracht, S. P. J.; Armstrong, F. A. J. *J. Am. Chem. Soc.* **2005**, *127*, 6595.
- (6) Stein, M.; van Lenthe, E.; Baerends, E. J.; Lubitz, W. *J. Am. Chem. Soc.* **2001**, *123*, 5839.
- (7) (a) Volbeda, A.; Charon, M. H.; Piras, C.; Fernandez, V. M.; Hatchikian, E. C.; Frey, M.; Fontecilla-Camps, J. C. *Nature* **1995**, *373*, 580. (b) Volbeda, A.; Garcin, E.; Piras, C.; de Lacey, A. L.; Fernandez, V. M.; Hatchikian, E. C.; Frey, M.; Fontecilla-Camps, J. C. *J. Am. Chem. Soc.* **1996**, *118*, 16988. (c) Volbeda, A.; Garcin, E.; Piras, C.; de Lacey, A. L.; Fernandez, V. M.; Hatchikian, E. C.; Frey, M.; Fontecilla-Camps, J. C. *J. Am. Chem. Soc.* **1996**, *118*, 12989.
- (8) (a) Siegbahn, P. E. M. *Adv. Inorg. Chem.* **2004**, *56*, 101. (b) Pavlov, M.; Blomberg, M. R. A.; Siegbahn, P. E. M. *Int. J. Quantum Chem.* **2004**, *56*, 101.
- (9) Amara, P.; Volbeda, A.; Fontecilla-Camps, J. C.; Field, M. J. *J. Am. Chem. Soc.* **1999**, *121*, 4468.
- (10) Thauer, R. K.; Klein, A. R.; Hartmann, G. C. *Chem. Rev.* **1996**, *96*, 3031.
- (11) Foerster, S.; Stein, M.; Brecht, M.; Ogata, H.; Higuchi, Y.; Lubitz, W. *J. Am. Chem. Soc.* **2003**, *125*, 83.
- (12) Hinnemann, B.; Moses, P. G.; Bonde, J.; Jørgensen, K. P.; Nielsen, J. H.; Hørch, S.; Chorkendorff, I.; Nørskov, J. K. *J. Am. Chem. Soc.* **2005**, *127*, 5308.
- (13) Ott, S.; Kritikos, M.; Akermark, B.; Sun, L. C.; Lomoth, R. *Angew. Chem., Int. Ed.* **2004**, *43*, 1006.
- (14) Borg, S. J.; Behrsing, T.; Best, S. P.; Razavet, M.; Liu, X. M.; Pickett, C. J. *J. Am. Chem. Soc.* **2004**, *126*, 16988.
- (15) Nguyen, D. H.; Hsu, H. F.; Millar, M.; Koch, S. A. *J. Am. Chem. Soc.* **1996**, *118*, 8963.

much simpler form.^{15,16} However, their catalytic activities for the HER have neither been studied in detail, nor been compared to those of the hydrogenases.

In the present study, density functional theory (DFT) was employed to describe the HER on the [NiFe] hydrogenase, plus the $[\text{Ni}(\text{PS3}^*)(\text{CO})]^{1-}$ and $[\text{Ni}(\text{PNP})_2]^{2+}$ complexes, in which Ni(II) is present. Ni(111) and Pt(111) single-crystal surfaces were also studied here as references. Through a mechanistic study of the HER on the hydrogenase and its analogues, we identify and analyze the function of the active sites, which helps to advance our understanding of how the biological system works. Furthermore, the configuration of the active sites also guides us to the selection of a new HER catalyst, the Ni_2P -(001) surface. Recent studies indicate that bulk Ni_2P is a very good catalyst for hydrodesulfurization (HDS) reactions and the production of hydrogen through the water–gas-shift (WGS) reaction.^{17,18} According to the present calculations, Ni_2P has the potential to be an excellent catalyst for the HER.

II. Theoretical Methods

Calculations were performed using spin-unrestricted DFT with the DMol³ code.¹⁹ The Kohn–Sham one-electron equations were solved on a double numerical basis set with polarization functions (DNP, local cutoff of 5.5 Å) of accuracy comparable to a Gaussian 6-31(d) basis. All of the electrons were used to describe the ionic cores.²⁰ For all of the surfaces investigated, we used a k-point sampling of $5 \times 5 \times 1$ Monkhorst–Pack special points²¹ in the *x*, *y*, and *z* directions, respectively. The exchange–correlation energy and the potential were described by the revised version of the Perdew–Burke–Ernzerhof (RPBE) functional.²² These setups have been proved very useful in theoretical studies dealing with metal surfaces, metal compound surfaces, and hydrogenases.^{12,23,24}

Bulk Pt and Ni have an fcc structure. Bulk Ni_2P adopts a hexagonal structure (see ref 24 for details). The optimized structural parameters for the bulk materials ($a = 3.97$ Å for Pt; $a = 3.56$ Å for Ni; $a = b = 5.93$ Å, $c = 3.37$ for Ni_2P) were in good agreement with experimental values ($a = 3.92$ Å for Pt;²⁵ $a = 3.52$ Å for Ni;²⁵ $a = b = 5.87$ Å, $c = 3.39$ for Ni_2P ²⁶). The surfaces were represented by a four-layer $\sqrt{3} \times \sqrt{3}$ (for $\text{Ni}_2\text{P}(001)$) or 2×2 (for Pt(111) and Ni(111)) unit cell. The interaction of H with the substrates at different coverage was investigated. In the calculations, the top three layers of the surfaces were allowed to relax in all dimensions together with the adsorbates, while the bottom layer was kept fixed at the calculated bulk positions. For the charged systems, DMol³ specifies the total charge on the molecule or enzyme unit. All of the atoms of the $[\text{Ni}(\text{PS3}^*)(\text{CO})]^{1-}$ and $[\text{Ni}(\text{PNP})_2]^{2+}$ complexes were allowed to relax with the bonded hydrogen species. In the case of the [NiFe] hydrogenase, we used the model employed in previous theoretical studies,^{8a} which includes the metal centers and key amino acids surrounding them. To prevent an

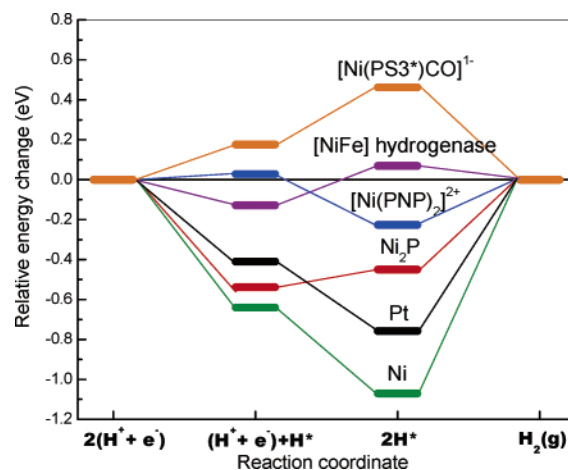


Figure 1. Calculated energy changes for the HER on the [NiFe] hydrogenase, the $[\text{Ni}(\text{PS3}^*)(\text{CO})]^{1-}$ and $[\text{Ni}(\text{PNP})_2]^{2+}$ complexes, plus Ni_2P -(001), Pt(111), and Ni(111) surfaces. The energy change for the $2(\text{H}^+ + \text{e}^-) \rightarrow \text{H}_2$ reaction is defined as zero by setting the reference potential to that of the standard hydrogen electrode.^{12,23} In the figure, we are plotting relative energy changes with respect to this zero of reference.

unrealistic movement of the second shell amino acid residues, one atom of each residue was frozen at the position found in the X-ray structure of the enzymes.^{8a} This method has been found to work very well in other studies.^{8a,27} For each optimized structure, a Mulliken population analysis²⁸ was carried out to estimate the partial charge on each atom and examine qualitative trends in charge redistribution.

III. Results and Discussion

HER follows either the Volmer–Tafel or the Heyrovsky mechanism. Recent experimental studies support the Volmer–Tafel mechanism in which two successive elementary steps are involved:^{16,29} an initial proton transfer to give bonded hydrogen atoms



followed by



where “*” represents a free active site on the system, and therefore “H*” stands for the hydrogen bonded to this site.

Combining the Volmer–Tafel mechanism and DFT calculations, we can elucidate the kinetics of the HER. By setting the reference potential to be that of the standard hydrogen electrode, the change in energy from $2(\text{H}^+ + \text{e}^-)$ to H_2 is defined as zero.^{12,23} Figure 1 displays the relative energy changes for the HER on a series of catalysts, involving the sequential adsorption of two hydrogens, followed by the desorption of H_2 into gas phase. In the present model, we only consider changes in energy, assuming that contributions to the entropy from vibrations are the same in all systems. This assumption is based on previous studies, which indicate a similar change in entropy and zero-point energy for hydrogen adsorption on metal surfaces, hydrogenases, and metal compounds.^{12,23} Therefore, taking into account the zero-point energy and the entropy will not affect the trend of the HER activity for these systems, which is our

- (16) Curtis, C. J.; Miedancer, A.; Ellis, W. W.; DuBois, D. L. *J. Am. Chem. Soc.* **2002**, *124*, 1918. Curtis, C. J.; Miedancer, A.; Ciancanelli, R.; Ellis, W. W.; Noll, B. C.; DuBois, M. R.; DuBois, D. L. *Inorg. Chem.* **2003**, *42*, 216.
- (17) Oyama, S. T. *J. Catal.* **2003**, *216*, 343.
- (18) (a) Sawhill, S. J.; Phillips, D. C.; Bussell, M. E. *J. Catal.* **2003**, *215*, 208. (b) Layman, K. A.; Bussell, M. E. *J. Phys. Chem. B* **2004**, *108*, 15791. (c) Gonzalez, L.; Liu, P.; Wang, X.; Hanson, J.; Bussell, M. E.; Rodriguez, J. A., to be published.
- (19) Delly, B. *J. Chem. Phys.* **1990**, *92*, 508; *J. Chem. Phys.* **2000**, *113*, 7756.
- (20) Vanderbilt, D. *Phys. Rev. B* **1990**, *41*, 7892.
- (21) Monkhorst, H. J.; Pack, J. D. *Phys. Rev. B* **1976**, *12*, 5188.
- (22) Hammer, B.; Hansen, L. B.; Nørskov, J. K. *Phys. Rev. B* **1999**, *59*, 7413.
- (23) Nørskov, J. K.; Bligaard, T.; Logadottir, A.; Kitchin, J. R.; Chen, J. G.; Pandelov, S.; Stimming, U. *J. Electrochem. Soc.* **2005**, *152*, J23.
- (24) (a) Liu, P.; Rodriguez, J. A.; Asakura, T.; Gomes, J.; Nakamura, K. *J. Phys. Chem. B* **2005**, *109*, 4575. (b) Rodriguez, J. A.; Kim, J. Y.; Hanson, J. C.; Sawhill, S. J.; Bussell, M. E. *J. Phys. Chem. B* **2003**, *107*, 6276.
- (25) <http://www.webelements.com/>.
- (26) Zonneville, M.; Hoffman, R.; Harris, S. *Surf. Sci.* **1998**, *199*, 320.

(27) Rodriguez, J. A.; Abreu, I. A. *J. Phys. Chem. B* **2005**, *109*, 2754.

(28) Mulliken, R. S. *J. Chem. Phys.* **1955**, *23*, 1833.

(29) Kunimatsu, K.; Senzaki, T.; Tsumihama, M.; Osawa, M. *Chem. Phys. Lett.* **2005**, *401*, 451.

interest here. On the surfaces, the first H adsorption (H^*) corresponds to a H coverage of 1/4 of a monolayer (ML) for Pt(111) and Ni(111), or 1/3ML for Ni₂P(001). The second addition of hydrogen ($2H^*$) corresponds to a coverage of 1/2ML or 2/3ML, respectively. Furthermore, as the proton and electron transfers are coupled together (eq 1), the charge of each system keeps constant during the HER.

In general, the good HER catalyst should be able to trap protons and bond the atomic hydrogen strongly, while still desorb H₂. Accordingly in Figure 1, the better catalyst corresponds to that with energy changes closer to the zero energy line. For the systems with one of the hydrogen trappings as the rate-limiting step (rls) (eq 1), the overall rate of HER at zero potential can be expressed as

$$r = k_{\text{rls}} \theta_* [\text{H}^+] = k_0 \exp\left(-\frac{\Delta E_a}{k_b T}\right) (1 - \theta_{\text{H}_I} - \theta_{\text{H}_{\text{II}}}) [\text{H}^+] \quad (3)$$

where k_{rls} and θ_* correspond to the rate constant of the rls and the concentration of free active sites in the catalyst, respectively. ΔE_a is the barrier for the rls. k_0 represents the prefactor for the rls. H_I and H_{II} stand for the first and second bonded hydrogen, respectively. Considering the very weak binding of hydrogen with these systems ($\theta_{\text{H}_I}, \theta_{\text{H}_{\text{II}}} \ll 1$), we obtain r at pH = 0 ($[\text{H}^+] = 1$) as

$$r \approx k_0 \exp\left(-\frac{\Delta E_a}{k_b T}\right) \quad (4)$$

We note here that the standard hydrogen electrode in electrochemical measurements is at pH = 0, but the hydrogenases work at pH = 7. Considering the usual compensation between the energy shifts introduced by the pH = 7 correction and by the redox potential for the electron transfer,³⁰ we neglect the pH dependence of eq 3 as done previously by other authors.¹² For the systems with the removal of the hydrogen as the rls (eq 2), the overall rate of the HER at zero potential is expressed as

$$r = k_{\text{rls}} \theta_{\text{H}_I} \theta_{\text{H}_{\text{II}}} = k_0 \exp\left(-\frac{\Delta E_a}{k_b T}\right) \theta_{\text{H}_I} \theta_{\text{H}_{\text{II}}} \quad (5)$$

In this case, considering strong hydrogen binding to the active sites ($\theta_{\text{H}_I} \theta_{\text{H}_{\text{II}}} \approx 1$), we again obtain r as

$$r \approx k_0 \exp\left(-\frac{\Delta E_a}{k_b T}\right) \quad (6)$$

Therefore, in both cases, the overall rate of the HER can be expressed, in a first approximation, as a function of the barrier for the rls. Considering the linear relationship between the reaction energy and the barrier with a ratio close to 1,^{31a} we use the reaction energy of the rls (ΔE_{rls}) in the following to estimate relative rates for the HER.^{31b,c} In fact, this hypothesis

was tested in our calculations, which give a near-linear correlation between ΔE_{rls} and ΔE_a for the HER on the [NiFe] hydrogenase, the [Ni(PS3*)(CO)]¹⁻, and [Ni(PNP)₂]²⁺ complexes with a slope of 0.84. That is, when ΔE_{rls} is lowered by 0.1 eV, the rate of HER increases by a factor of 26 at pH = 0 and room temperature.

A. HER on Pt(111) and Ni(111) Surfaces. Pt is usually an electrode catalyst used in the photoconversion of water to hydrogen.² As shown in Figure 1, Pt and Ni are two of the worst HER catalysts in the present study, corresponding to an energetics far away from the ideal zero line.¹² The atoms in Pt(111) and Ni(111) surfaces have a small negative charge (Pt, -0.1e; Ni, -0.05e) and behave as proton acceptors. One can see in Figure 1 that the first (H^*) and second ($2H^*$) hydrogen trappings on both metal surfaces are exothermic, and the recombination and removal of H₂ (eq 2) is the rls for the HER. In the case of pure Ni, the bonding strengths of the first (E_{H_I} , at coverage of 1/4ML) and second H ($E_{\text{H}_{\text{II}}}$, at coverage of 1/2ML) are very strong: -0.64 and -0.43 eV, respectively. As a result, the removal of hydrogen becomes highly endothermic ($\Delta E_{\text{rls}} = 1.07$ eV, Figure 1), and the HER cannot proceed well. Turning to the less reactive pure Pt, E_{H_I} decreases to -0.41 eV, which is in reasonable agreement with a previously calculated value of -0.33 eV.²³ In addition, $E_{\text{H}_{\text{II}}}$ also decreases (-0.35 eV), and, consequently, ΔE_{rls} is lowered by 0.31 eV. This indicates that Pt is a better HER catalyst than Ni, which was also observed in other studies.^{12,23} However, we notice in Figure 1 that to remove H from a Pt(111) surface, the energy cost is still relatively high ($\Delta E_{\text{rls}} = 0.76$ eV). Therefore, searching for new HER catalysts is a clear need.

B. HER on the [NiFe] Hydrogenase. As shown in Figure 1, in accordance with the experiments,⁴⁻⁹ the [NiFe] hydrogenase is superior to Pt as an HER catalyst with only a 0.2 eV cost for the rls. To describe HER on a [NiFe] hydrogenase, we start with its geometry. There have been a number of studies to clarify the structure of the [NiFe] hydrogenase in both theory and experiment.^{6-8,32-35} As shown in Figure 2, the model from Siegbahn was employed in the present study with an overall charge of -2e.^{8a} This model has proved to be quite useful to describe the kinetics of H₂ oxidation.⁸ The Ni atom is coordinated to the sulfur atoms of four cysteine residues. Two of them act as a bridge between Ni and Fe (S_b), and two of them are bound to Ni as terminal cysteines (S_t). The Fe is further bonded to three inorganic diatomic ligands, one CO and two CN⁻. As shown in Table 1, the geometric parameters of the [NiFe] hydrogenase obtained in the present calculations are in reasonable agreement with those determined from experiments of EXAFS³³ or X-ray diffraction (XRD)³⁴ and predicted by other DFT calculations.³⁵

Figure 3 displays the calculated electron density for the hydrogenase. In principle, all blue regions (highly negative charge) may become the proton acceptor. However, as indicated in ref 8a, only the O of Glu23 (-0.44e) and N of His77 (-0.34e) are exposed to the medium for trapping protons, and according

(30) Teixeira, M.; Moura, I.; Xavier, A. V.; Moura, J. J. G.; LeGall, J.; DerVartanian, D. V.; Peck, H. D., Jr.; Huynh, B. H. *J. Biol. Chem.* **1989**, *264*, 16435.

(31) (a) Nørskov, J. K.; Bligaard, T.; Logadottir, A.; Bahn, S.; Hansen, L. B.; Bollinger, M.; Bengard, H.; Hammer, B.; Sljivancanin, Z.; Mavrikakis, M.; Xu, Y.; Dahl, S.; Jacobsen, C. J. H. *J. Catal.* **2002**, *209*, 275. (b) Schumacher, N.; Boisen, A.; Dahl, S.; Gokhale, A. A.; Kandoi, S.; Grabow, L. C.; Dumesic, J. A.; Mavrikakis, M.; Chorkendorff, I. *J. Catal.* **2005**, *229*, 265. (c) Liu, P.; Logadottir, A.; Nørskov, J. K. *Electrochim. Acta* **2003**, *48*, 3731.

(32) Bruschi, M.; Fantucci, P.; de Goia, L. *Inorg. Chem.* **2004**, *43*, 3733.

(33) Gu, W.; Jacquamet, J.; Patil, D. S.; Wang, H.-X.; Evans, D. J.; Smith, M. C.; Millar, M.; Koch, S.; Eichhorn, D. M.; Latimer, M.; Cramer, S. P. *J. Inorg. Biochem.* **2003**, *93*, 41.

(34) Hoguchi, Y.; Ogata, H.; Miki, K.; Yasuoka, N.; Yagi, T. *Struct. Folding Des.* **1999**, *7*, 549.

(35) De Goia, L.; Fantucci, P.; Guigliarelli, B.; Bertrand, P. *Inorg. Chem.* **1999**, *38*, 2658.

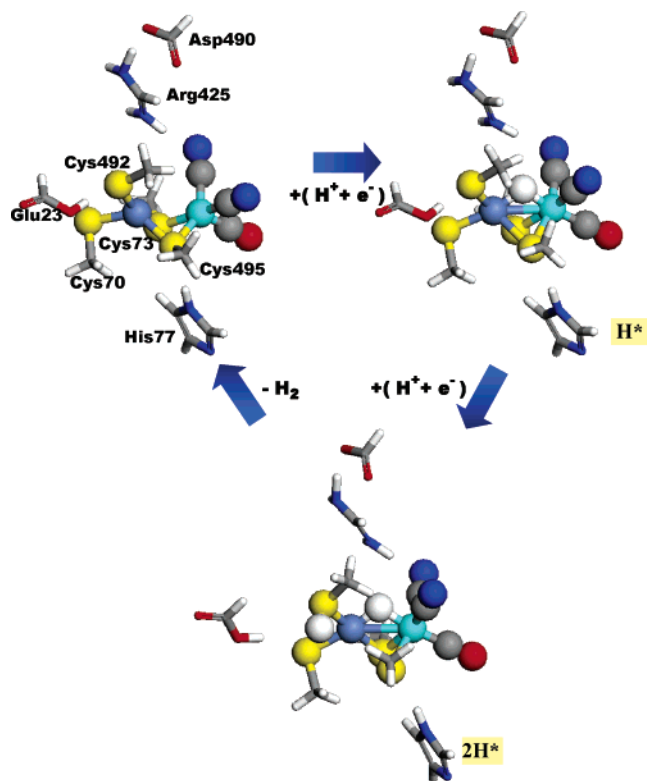


Figure 2. Optimized structures for each step in a catalytic cycle for the HER on the [NiFe] hydrogenase (white, H; gray, C; navy, Ni; cyan, Fe; blue, N; red, O; yellow, S).

Table 1. Comparison of Selected Bond Distances for the [NiFe] Hydrogenase^a

	EXAFS ³³	XRD ³⁴	DFT (BLYP) ³⁵	DFT (this work)
Ni–Fe	2.54	2.59	2.67	2.63
Ni–S _t	2.21	2.24	2.39	2.24
Ni–S _i	2.21	2.32	2.33	2.29
Ni–S _b	2.47	2.33	2.46	2.40
Ni–S _b	2.47	2.43	2.58	2.53

^a See the text and Figure 2 for the labeling of the atoms.

to our calculations the former is the most stable site for attracting protons from the solution. Once the proton attacks this O, the O–H bond close to the core breaks, and the H forms an H–S bond with the terminal S of Cys492. With the electron transfer, the atomic H favors bonding to Ni–Fe bridge sites (hydride acceptors), with an energy gain of 0.13 eV (*H, Figure 2), which is also observed in the other theoretical studies.^{6,8a,12} Therefore, there should be a sequential migration of H from the Cys492 to the Ni–Fe bridge.

The rls for the HER on the [NiFe] hydrogenase is the addition of the second atomic hydrogen. As the first hydrogen atom has occupied a hydride-acceptor site, fitting the additional one at the same site 1.5 Å apart leads to the formation of dihydrogen (H–H bond length of 0.86 Å) sticking to the Ni, with a ΔE_{rls} of 0.43 eV. Instead, the second H prefers staying at the terminal S of Cys492 (bottom of Figure 2), accompanied by the ΔE_{rls} decreasing to 0.2 eV. In contrast, the removal of hydrogen is exothermic ($\Delta E_{\text{rls}} = -0.07$ eV, Figure 1). Our calculations also show that the dihydrogen bonded with Fe is not stable and shifts to the Ni site spontaneously (H*, Figure 2). To interact with dihydrogen, the metal sites have to transfer electrons to hydrogen. Fe with a bigger positive charge does not bind

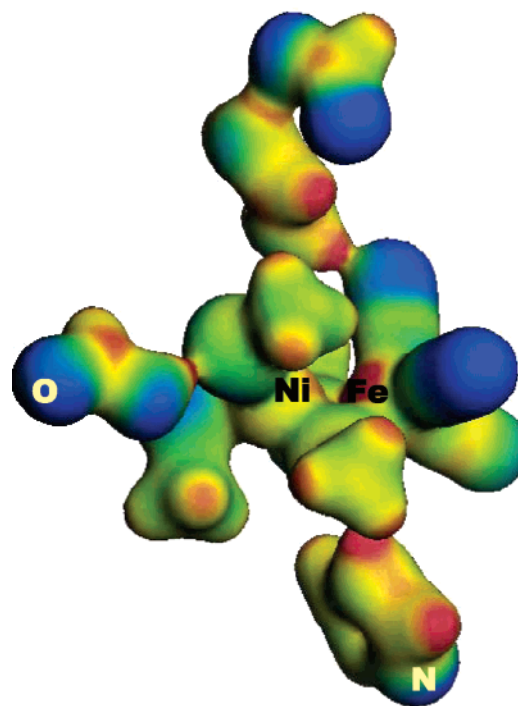


Figure 3. Calculated total electron density of the [NiFe] hydrogenase mapped by the electrostatic potential. The isosurface value is $0.2 \text{ e } \text{Å}^{-3}$. Electrostatic potential is color coded as follows: the blue corresponds to negatively charged regions, while the red represents positively charged regions.

dihydrogen as strongly as Ni. On the other hand, the coordination number of Fe is five, while Ni only has four ligands (Figure 2) and therefore less steric repulsion toward dihydrogen. Overall, our calculations show that the Ni site of the hydrogenase plays an essential role in the HER. This is in agreement with experimental observations that point to Ni as the active site for the reaction with hydrogen.³⁶

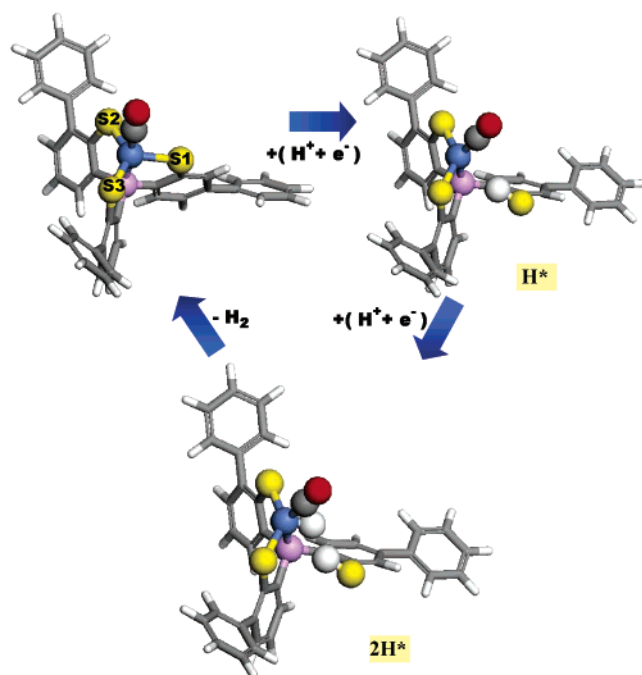
C. HER on the [Ni(PS3*)(CO)]¹⁻ and [Ni(PNP)₂]²⁺ Complexes. Considering the activity of Ni sites under different chemical environments, we are interested in the HER on the two Ni complexes, [Ni(PS3*)(CO)]¹⁻ and [Ni(PNP)₂]²⁺, that are analogues of the hydrogenase.^{15,16} These complexes also include proton- and hydride-acceptor sites. Besides, they have a smaller size and are more tunable than the hydrogenase enzyme, which is attractive for fundamental research and practical applications.^{15,16} Similarly to the hydrogenases, the present study does not include the solvation effect for the two complexes. We assume that the effect of solvation on the energetics by changing the pH value can be neglected as is the case for the hydrogenases.³⁰ In the following, we will see that the present calculations give the molecular geometries in good agreement with the experimental data.

According to our results in Figure 1, the [Ni(PS3*)(CO)]¹⁻ complex displays a HER activity that is much worse than that of the hydrogenase, with a cost of 0.31 eV for the rls. As listed in Table 2, our calculated structure for [Ni(PS3*)(CO)]¹⁻ in Figure 4 is in good agreement with the XRD measurement,

(36) Montet, Y.; Amara, P.; Volbeda, A.; Vernede, A.; Hatchikian, E. C.; Field, M. J.; Fontecilla-camoes, J. C. *Nat. Struct. Biol.* **1997**, *4*, 523. Amara, P.; Volbeda, A.; Fontecilla-camoes, J. C.; Field, M. J. *J. Am. Chem. Soc.* **1999**, *121*, 4468. Stadler, C.; de Lacey, A. L.; Montet, Y.; Volbeda, A.; Vernede, A.; Fontecilla-camoes, J. C.; Conesam, J. C.; Fernandez, V. M. *Inorg. Chem.* **2002**, *41*, 4424.

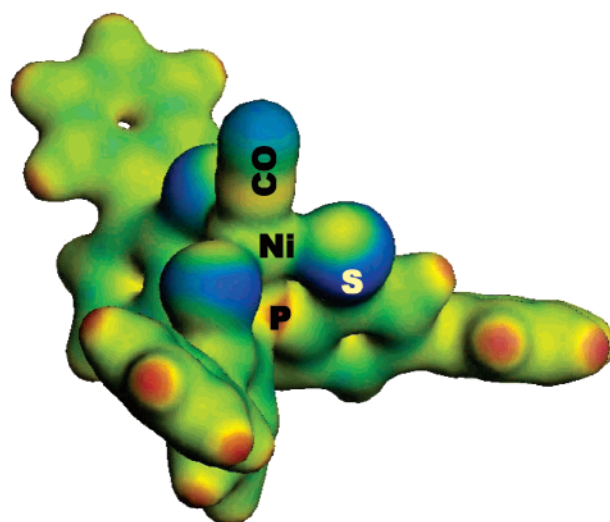
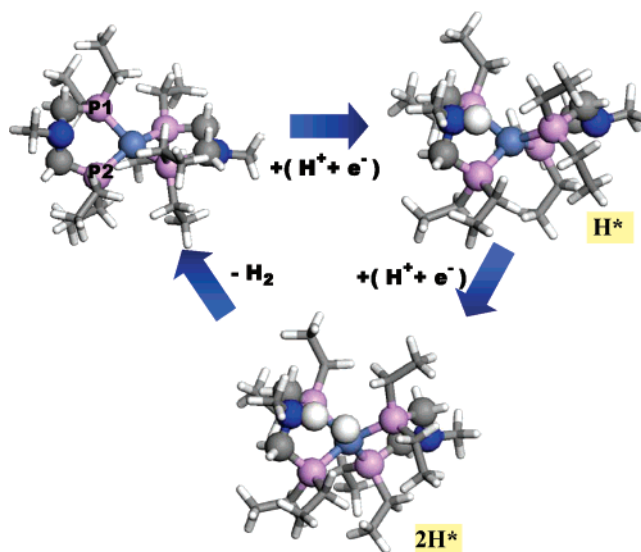
Table 2. Comparison of Selected Bond Distances for the $[\text{Ni}(\text{PS3}^*)(\text{CO})]^{1-}$ Complex^a

	XRD ¹⁵	DFT (this work)
Ni–S1	2.35	2.40
Ni–S2	2.27	2.30
Ni–S3	2.31	2.33
Ni–C	1.75	1.80
Ni–P	2.09	2.14
C–O	1.15	1.16

^a See Figure 4 for the labeling of the atoms.**Figure 4.** Optimized structures for each step in a catalytic cycle for the HER on the $[\text{Ni}(\text{PS3}^*)(\text{CO})]^{1-}$ complex (white, H; gray, C; navy, Ni; purple, P; blue, N; red, O; yellow, S).

corresponding to a distorted trigonal bipyramidal structure with the CO in the axial position trans to the P atom.¹⁵ One can see in Figure 5 that the S sites are negatively charged (~ -0.4 eV) and become the proton-acceptor sites as the O of Glu23 in the $[\text{NiFe}]$ hydrogenase. With H attacking S ($\Delta E = 0.18$ eV), the Ni–S bond spontaneously breaks and the formed HS group is bonded to only the benzene ring (H^* , Figure 4). The binding energy of H with the Ni site is 0.71 eV weaker. This is due to the strong Ni–S interactions in $[\text{Ni}(\text{PS3}^*)(\text{CO})]^{1-}$ (Figure 4). As a result, we observe in the calculations that Ni has to break one of its Ni–S bonds to be able to interact with one H atom. Similarly to the hydrogenase, the addition of the second H is the rls for the HER on $[\text{Ni}(\text{PS3}^*)(\text{CO})]^{1-}$. With the decrease in the Ni coordination in the first step (H^* , Figure 4), the second H favors bonding to the Ni site, corresponding to a ΔE_{rls} of 0.31 eV (2H^* , Figure 4), which is lower than that for the hydrogenase. Due to the weak interaction, the hydrogen removal from $[\text{Ni}(\text{PS3}^*)(\text{CO})]^{1-}$ is exothermic ($\Delta E = -0.49$ eV).

Our calculations indicate that the $[\text{Ni}(\text{PNP})_2]^{2+}$ complex catalyzes the HER quite well with the energy required for the rls being only 0.23 eV, a value comparable to that of the $[\text{NiFe}]$ hydrogenase (Figure 1). Following the XRD studies,¹⁶ a tetrahedrally distorted square plane was considered for $[\text{Ni}(\text{PNP})_2]^{2+}$ in the present study (Figures 6 and 7). Our optimized structure is in good agreement with the structure derived from

**Figure 5.** Calculated total electron density of the $[\text{Ni}(\text{PS3}^*)(\text{CO})]^{1-}$ complex mapped by the electrostatic potential. The isosurface value is $0.2 \text{ e } \text{Å}^{-3}$. Electrostatic potential is color coded as follows: the blue corresponds to negatively charged regions, while the red represents positively charged regions.**Figure 6.** Optimized structures for each step in a catalytic cycle for the HER on the $[\text{Ni}(\text{PNP})_2]^{2+}$ complex (white, H; gray, C; navy, Ni; purple, P; blue, N).

an XRD study (Table 3).¹⁶ The calculated dihedral angle between the two planes defined by the two P atoms of each chelating diphosphine ligand and Ni is 36.5° , a value close to the experimental measurement (34.1°).¹⁶ Nitrogen, with a negative charge of $-0.34e$, behaves as the proton acceptor. In contrast, the highly coordinated P and Ni sites are positively charged and cannot stabilize the proton, which shifts to the N sites spontaneously. According to our calculations, the first bonded H favors the N site of the complex (H^* , Figure 6) rather than the Ni site by 0.17 eV, while the second one prefers the Ni site rather than the N sites by 0.08 eV. Therefore, we propose a sequential migration of the bonded H from N to Ni ($[\text{HNi}(\text{PNP})(\text{PNHP})]^{2+} \rightarrow [\text{HNi}(\text{PNP})(\text{PNHP})]^{2+}$). Note that the two H atoms have opposite charges. A charge of $0.3e$ was observed for the one bonded to the N site and $-0.16e$ for the other at the Ni site. Therefore, one can see in Figure 6 that, once the migration is completed, the two H atoms attract each other and

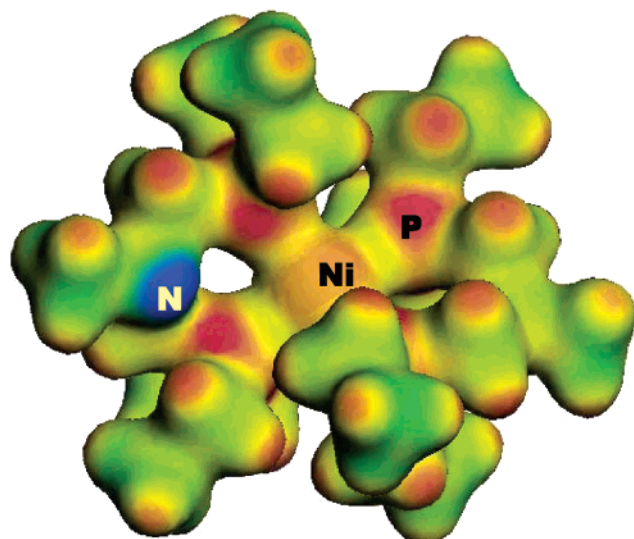


Figure 7. Calculated total electron density of the $[\text{Ni}(\text{PNP})_2]^{2+}$ complex mapped by the electrostatic potential. The blue corresponds to negatively charged regions, while the red indicates positively charged regions.

Table 3. Comparison of Selected Bond Distances for the $[\text{Ni}(\text{PNP})_2]^{2+}$ Complex^a

	XRD ¹⁶	DFT (this work)
Ni–P1	2.23	2.30
Ni–P2	2.24	2.31

^a See Figure 6 for the labeling of the atom.

form a weak H–H bond with a bond length of 1.55 Å, a possible precursor for the formation of H₂. Similar to the Ni and Pt surfaces, the rls of the HER on $[\text{Ni}(\text{PNP})_2]^{2+}$ is also the recombination and removal of hydrogen. However, in this case the energy cost is only 0.23 eV.

As demonstrated above, when compared to the $[\text{NiFe}]$ hydrogenase and its molecular analogues, bulk Pt or Ni catalyzes the HER less efficiently, as hydrogen bonds too strongly with Pt to be removed from the surface efficiently. The hydrogenase and its analogues include both a proton acceptor (a negatively charged nonmetal site) to strongly trap the protons, and a hydride acceptor (usually the highly coordinated and isolated metal site) to provide moderate bonding to the hydrogen. With the cooperative function of these two kinds of sites, the $[\text{NiFe}]$ hydrogenase displays a high catalytic activity in the HER. However, it has been found that under conditions different from their native environment, the $[\text{NiFe}]$ hydrogenase may lose activity due to a lack of thermostability, which hinders the application of this enzyme or the Fe-only hydrogenase in industrial processes.^{37,38} Therefore, Pt is still widely used as an industrial catalyst for the HER,² and there is a need to find a better alternative. In the following, we take a step further in the search for a material that combines the catalytic activity of the $[\text{NiFe}]$ hydrogenase and the thermostability of the metal surfaces.

D. HER on a Ni₂P(001) Surface. In Ni₂P, the concentration of Ni is diluted by the presence of P, and the formation of Ni–P bonds induces relatively minor perturbations in the electronic

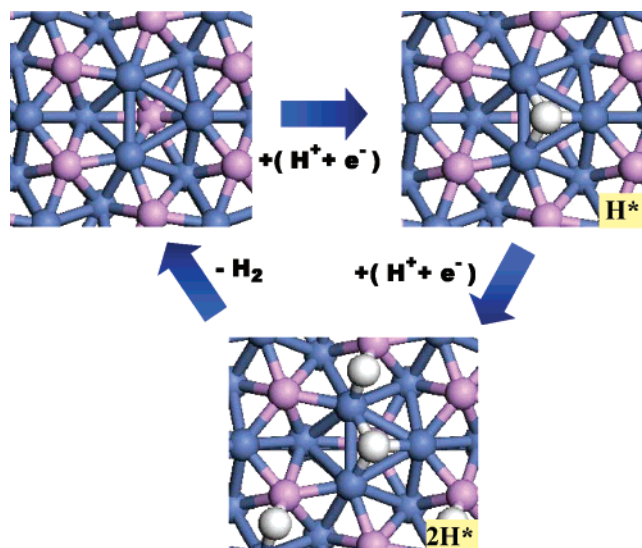


Figure 8. Optimized structures for each step in a catalytic cycle for the HER on a Ni₂P(001) surface (white, H; navy, Ni; purple, P).

properties of nickel.²⁴ Ni₂P(001) is a Ni₃P₂-terminated surface with alternating Ni₃P and Ni₃P₂ planes to give the full stoichiometry of the bulk along the [001] direction (Figure 8).²⁴ It has been found that the supported Ni₂P exhibits an extremely high HDS activity, corresponding to a conversion of 99%.^{17,18} The high catalytic activity of Ni₂P is ascribed to the complex role of P. First, the formation of Ni–P bonds produces a weak “ligand effect” (minor stabilization of the Ni 3d levels and a small Ni→P charge transfer) that allows a high activity for the dissociation of thiophene and molecular hydrogen. Second, the number of active Ni sites present in the surface decreases due to an “ensemble effect” of P, which prevents the system from the deactivation induced by high coverages of strongly bound S. Furthermore, the P sites are not simple spectators and provide moderate bonding to the products of the decomposition of thiophene and the H adatoms necessary for hydrogenation.²⁴

The Ni₂P(001) system seems to meet the criteria of a good HER catalyst, combining the best features of surfaces, the $[\text{NiFe}]$ hydrogenase, and the molecular complexes. On one hand, Ni₂P(001) is a solid surface as Pt(111) and Ni(111) and should have a higher thermostability than hydrogenase enzymes. In addition, due to the presence of the P atom in the surface, Ni₂P(001) behaves somewhat like the hydrogenase rather than the pure metal surfaces. One can see in Figure 9 that the Ni₂P(001) surface also includes the proton-acceptor (P sites) and hydride-acceptor centers (Ni site). P in the surface has a small negative charge of $-0.07e$ and can trap protons as the bases in the hydrogenase and the complexes, although it is not a strong base. For hydrogen, the Ni hollow sites are highly preferred ($E_{\text{H}_1} = -0.54$ eV at coverage of 1/3ML), as observed in the cases of Pt(111) and Ni(111). Due to a weak ligand effect,²⁴ the deactivation of Ni atoms in the surface of Ni₂P(001) is very small and the Ni hollow sites are strong hydride acceptors. Therefore, it is observed in Figure 1 that the first H adsorption (H*) on Ni₂P(001) is slightly weaker than that on Ni(111) but stronger than that on Pt(111), the hydrogenase, and the molecular complexes. Different from the pure metal surfaces, the addition of the second atomic hydrogen (2H*) on Ni₂P(001) is an endothermic process ($E_{\text{H}_2} = 0.09$ eV at coverage of 2/3ML). This endothermicity is due to an ensemble effect. As shown in

(37) Eijssink, V. G. H.; Bjørk, A.; Gåseidnes, S.; Sirevåg, R.; Synstad, B.; van den Burg, B.; Vriend, G. *J. Biotechnol.* **2004**, *113*, 105.

(38) Korkegain, A.; Black, M. E.; Baker, D.; Stoddard, B. L. *Nature* **2005**, *308*, 857.

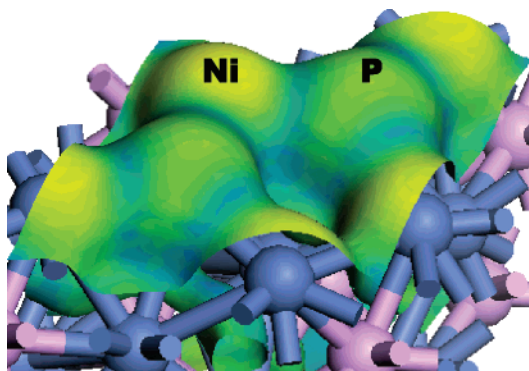


Figure 9. Calculated total electron density of a Ni₂P(001) surface mapped by the electrostatic potential. The isosurface value is 0.2 e Å⁻³. Electrostatic potential is color coded as follows: the blue corresponds to negatively charged regions, while the red represents positively charged regions.

Figure 8, once the Ni hollow sites have been occupied, the additional adsorbate has to interact with the less active Ni–P bridge site. As a result, the rls, that is, the removal of H₂ from Ni₂P(001), becomes less energy-consuming ($\Delta E_{\text{rls}} = 0.45$ eV), as compared to the cases of Ni(111) and Pt(111). Note that, according to our calculations, the Ni–P bridge site is the preferential site for the H adsorption on the Ni₂P(001) surface after occupying Ni hollow sites. This highlights that the P sites are not simple spectators and provide moderate bonding to important intermediates involved in the HER. Overall, we can see in Figure 1 that the catalytic activity of the Ni₂P(001) surface toward the HER should be better than those of Pt (111) and Ni(111), but worse than those of the [NiFe] hydrogenase and the [Ni(PNP)₂]²⁺ complex.

An important issue concerning the practical application of Ni₂P as an electrocatalyst is whether hydrogen and water might cover permanently the Ni sites under working conditions. According to our calculations, water adsorbs weakly on the Ni₂P(001) surface even at the Ni hollow site (−0.22 eV), and the reaction of water dissociation



is thermoneutral (−0.04 eV) and corresponds to an adsorption free energy of ~0.31 eV according to ref 23. Experiments for the bonding of water to Ni₂P(001) show that the molecule adsorbs intact and desorbs at temperatures between 150 and 180 K with a binding energy of 0.2–0.3 eV.³⁹ In contrast, the interaction of hydrogen with the Ni hollow sites of Ni₂P(001) is much stronger. The H removal in the form of H₂ is highly endothermic and costs the energy of 1.08 eV.²³ Therefore, it seems that H rather than water or the products from water dissociation may be bonded to the Ni₂P(001) surface. In fact, the strong interaction of H with the Ni hollow sites can lead to poisoning of the most chemically active part of the surface under the real working conditions for the HER.

Now the question is whether the H-poisoned Ni₂P(001) surface is able to catalyze the HER. Figure 10 plots the calculated relative rate for the HER (Δr) on the poisoned Ni₂P(001) and Pt(111) surfaces at pH = 0, zero potential, and room temperature. Here, all of the catalysts shown in Figure 1 are also included for comparison. Using eqs 4 and 6, Δr is expressed relative to the case of clean Pt(111) as

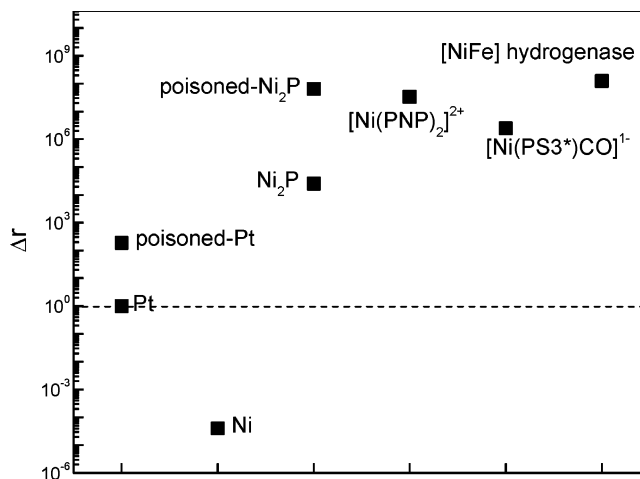


Figure 10. Calculated relative rate of the HER (Δr) on the H-poisoned Ni₂P(001) and Pt(111) surfaces as well as the catalysts displayed in Figure 1 at pH = 0, zero potential, and room temperature. Here, the HER rate is expressed relative to the case of Pt(111) following eq 8. The H-poisoned Ni₂P(001) surface contains 1/3 of a H monolayer occupying the three-fold Ni hollow sites, and 1/4 of a H monolayer bonded to Pt hollow sites in the case of the H-poisoned Pt(111).

$$\Delta r = \frac{r}{r_{\text{Pt}}} \approx \exp\left(-\frac{E_a - E_a^{\text{Pt}}}{k_{\text{B}}T}\right) \quad (8)$$

The corresponding optimized geometry of the intermediates involved in the HER of the H-poisoned Ni₂P(001) surface is displayed in Figure 11. One can see that with the Ni hollow sites occupied, the HER on Ni₂P(001) occurs at two Ni–P bridge sites, and the bonding to the first (2/3ML) and second H (1ML) atoms becomes endothermic, with E_{H_1} and E_{H_2} of 0.09 and 0.21 eV, respectively. Similar to the [NiFe] hydrogenase, our results show that the rls of the HER on the H-poisoned Ni₂P(001) surface is the addition of the second hydrogen (2H*, Figure 11). In Figure 10, the corresponding reaction energy of the rls ($\Delta E_{\text{rls}} = 0.21$ eV, $\Delta r \approx 6.5 \times 10^7$) is energetically between those of the [Ni(PNP)₂]²⁺ complex ($\Delta E_{\text{rls}} = 0.23$ eV, $\Delta r \approx 3.4 \times 10^7$) and the [NiFe] hydrogenase ($\Delta E_{\text{rls}} = 0.19$ eV, $\Delta r \approx 1.2 \times 10^8$). This indicates that the H poisoning of the Ni₂P(001) surface does not deactivate the catalyst at all; instead, ΔE_{rls} is lowered by 0.24 eV and the HER rate becomes comparable to that of the hydrogenase. In fact, it has also been found experimentally that Ni₂P exhibits a high stability and a sustained high activity for hydrodesulfurization processes (500–700 K and S-rich) and for the production of hydrogen through the water–gas-shift reaction (CO, H₂O, H₂-rich).^{17,18} Thus, it is likely that Ni₂P would perform well as a catalyst for the electrochemical evolution of hydrogen.

We also studied the H-poisoning of Pt(111). H adsorption on Pt(111) is weaker than that on Ni₂P(001) by 0.13 eV (Figure 1), and poisoning by the adsorbate should be less probable than in the case of Ni₂P(001). With 1/4ML of H-poisoning (Figure 10), our calculations predict an enhanced activity of Pt(111), due to the decreased H binding energy (E_{H_1} , −0.35 eV at coverage of 1/2ML; E_{H_2} , −0.26 eV at coverage of 3/4ML). Although the H–Pt bonding at high coverage is not strong enough to cover the whole surface, ΔE_{rls} is still relatively high (0.6 eV, $\Delta r \approx 1.9 \times 10^2$) and the promotion by H poisoning of Pt(111) is not as significant as that of Ni₂P(001). As shown in Figure 1, to accelerate the HER on Pt and Ni₂P, one has to

(39) Ogata, T.; Nakamura, K.; Liu, P.; Rodriguez, J. A., to be published.

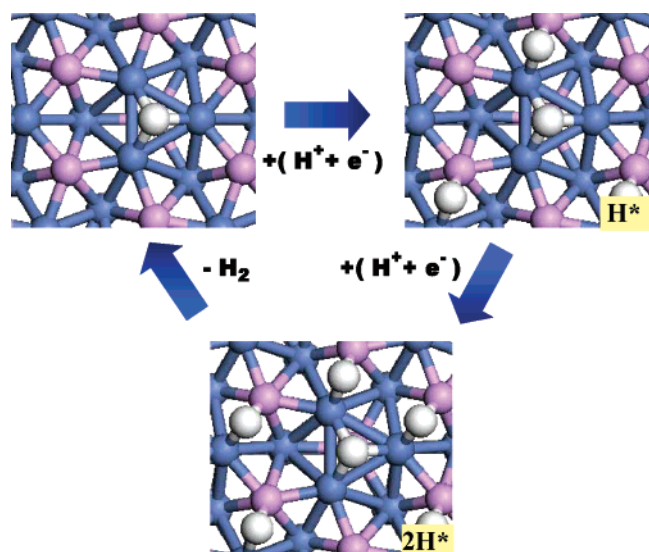


Figure 11. Optimized structures for each step in a catalytic cycle for the HER on a H-poisoned $\text{Ni}_2\text{P}(001)$ surface (white, H; navy, Ni; purple, P). Initially, the three-fold Ni hollow sites are occupied by atomic H.

decrease their interactions with hydrogen. On the clean $\text{Ni}_2\text{P}(001)$ surface (Figure 8), the Ni hollow sites bond the hydrogen most strongly. Due to an ensemble effect, the number of metal hollow sites on $\text{Ni}_2\text{P}(001)$ is greatly decreased as compared to that of $\text{Ni}(111)$ and $\text{Pt}(111)$, and 1/3 of a H monolayer has blocked all of the active metal hollow sites. In this way, the H-poisoned $\text{Ni}_2\text{P}(001)$ surface is forced to bond the intermediates and products moderately at the less active Ni–P bridge sites (Figure 11), and therefore the HER becomes more facile. In the case of $\text{Pt}(111)$, even with 1/4 of a monolayer of H-poisoning, there are still plenty of Pt hollow sites available to adsorb hydrogen more strongly than that of $\text{Ni}_2\text{P}(001)$. Consequently, the weakening of the H–Pt bond is relatively small.

Overall, our DFT calculations show that the $\text{Ni}_2\text{P}(001)$ surface should display a better catalytic activity toward the HER than the conventional catalyst Pt. As compared to the [NiFe] hydrogenase and the analogue complexes $[\text{Ni}(\text{PS}_3^*)(\text{CO})]^{1-}$ and $[\text{Ni}(\text{PNP})_2]^{2+}$, the HER on pure $\text{Ni}_2\text{P}(001)$ is less efficient, due to the fact that Ni sites of $\text{Ni}_2\text{P}(001)$ bond hydrogen too strongly hindering its removal from the surface. The H-poisoned $\text{Ni}_2\text{P}(001)$ surface should catalyze the HER with an efficiency comparable to that of the [NiFe] hydrogenase. Different from the HDS catalysis,²⁴ the weak ligand effect of P on Ni does not contribute to the good behavior of Ni_2P toward the HER. If considering only the ligand effect of Ni_2P , the HER activity of the systems in this study should decrease in a sequence: [NiFe] hydrogenase > $[\text{Ni}(\text{PNP})_2]^{2+}$ > $[\text{Ni}(\text{PS}_3^*)(\text{CO})]^{1-}$ > Pt > Ni_2P > Ni. In fact, it is the ensemble effect that plays an essential role for the high activity of Ni_2P toward the HER. The energy cost for hydrogen removal (rls) from Ni_2P is decreased by

binding the second H atom at Ni–P bridge sites, and the activity decreases follow the sequence: [NiFe] hydrogenase > $[\text{Ni}(\text{PNP})_2]^{2+}$ > $[\text{Ni}(\text{PS}_3^*)(\text{CO})]^{1-}$ > Ni_2P > Pt > Ni (Figure 1). In fact, the promotion of Ni_2P toward the HER becomes more pronounced in the case of a H-poisoned surface (Figure 10), in which the reaction occurs over two Ni–P bridges sites with an efficiency comparable to that of the [NiFe] hydrogenase.

An important point in this study is that surfaces of pure transition metals do not have the necessary chemical properties for being highly active catalysts for hydrogen evolution. Such catalysts must have a moderate interaction with hydrogen species, combining proton-acceptor sites (negative charged nonmetal atoms) and hydride-acceptor sites (isolated metal atoms) that work in a cooperative way. Given these requirements, even alloys of transition metals with inert metals (Cu, Ag, Au) may not work well, and the logical focus of the search for highly active HER catalysts should be on compounds of transition metal with light elements.

IV. Conclusion

DFT-GGA calculations were employed to investigate the HER activity of the [NiFe] hydrogenase, $[\text{Ni}(\text{PS}_3^*)(\text{CO})]^{1-}$, $[\text{Ni}(\text{PNP})_2]^{2+}$, $\text{Ni}(111)$, $\text{Pt}(111)$, and $\text{Ni}_2\text{P}(001)$. Our results show that the [NiFe] hydrogenase exhibits the highest activity for the HER, followed by $[\text{Ni}(\text{PNP})_2]^{2+}$ > Ni_2P > $[\text{Ni}(\text{PS}_3^*)(\text{CO})]^{1-}$ > Pt > Ni in a decreasing sequence. Among the bulk surfaces, $\text{Ni}_2\text{P}(001)$ displays a superior activity over the conventional Pt catalyst. Nevertheless, the HER on the surfaces is slower than those on the hydrogenase and $[\text{Ni}(\text{PNP})_2]^{2+}$ due to the fact that the metal sites bond hydrogen too strongly to allow the facile removal of H_2 . Our calculations also show that with 1/3 of a monolayer of H poisoning the hollow sites of $\text{Ni}_2\text{P}(001)$, the poisoned surface displays a high HER activity comparable to those of the [NiFe] hydrogenase and the $[\text{Ni}(\text{PNP})_2]^{2+}$ complex. According to our DFT calculations, Ni_2P should be the best practical catalyst for the HER among all of these systems, combining the high thermostability of extended surfaces and the high catalytic activity of the hydrogenase.

The good behavior of Ni_2P is associated with an ensemble effect, where the concentration of highly active Ni sites in the surface is decreased by the presence of P. In addition, the P sites are not simple spectators and provide moderate bonding to the reaction intermediates. As a result of these, the surface has proton-acceptor and hydride-acceptor centers that work to facilitate the HER.

Acknowledgment. The research carried out at Brookhaven National Laboratory was supported by the U.S. Department of Energy, Division of Chemical Sciences, under contract DE-AC02-98CH10886.

JA0540019